SUPPLEMENTARY INFORMATION: Empirical evidence and theoretical understanding of ecosystem carbon and nitrogen cycle interactions

Benjamin D. Stocker, Ning Dong, Evan A. Perkowski, Pascal D. Schneider, Huiying Xu, Hugo de Boer, Karin T. Rebel, Nicholas G. Smith, Kevin Van Sundert, Han Wang, Sarah E. Jones, I. Colin Prentice and Sandy P. Harrison

Contents

S1 Analysis of modelled land C sink trends

We evaluated the time series of the simulated and observations-based land C balance, its decadal mean for years 2011-2020 and long-term trend for years 1959-2020 from outputs of the Trends and Drivers of Terrestrial Sources and Sinks of Carbon Dioxide (TRENDY) version 8 model intercomparison (Sitch et al., 2024). We downloaded the original file `Global_Carbon_Budget_2021v1.0.xlsx` (`doi:10.18160/gcp-2021`) from the Global Carbon Budget 2021 website and exported the tabs 'Terrestrial Sink' and 'Global Carbon Budget' for further analysis. From the latter, we derived the land C sink as the budget residual as quantified by (Friedlingstein et al., 2022):

$$S_{\text{Land}} = (E_{\text{FF}} + E_{\text{LUC}}) - (G_{\text{atm}} + S_{\text{ocean}} + S_{\text{cement}}) \,, \tag{S1}$$

where S_{Land} is the land sink ('Observations' in Fig. 1 of the main text), E_{FF} are emission from fossil fuel combustion, E_{LUC} are emissions from land use change, G_{atm}

is the atmospheric growth rate, S_{ocean} is the ocean sink, and S_{cement} is the C sink from cement carbonation. The land sink simulated by models was taken as the annual C flux numbers provided in the tab 'Terrestrial Sink' of the original file. It was taken by (Friedlingstein et al., 2022) as the global biome producitivity (net terrestrial C balance) from simulations (TRENDY S2) forced by observed CO_2 and climate and with constant pre-industrial land use. The identification of models into C-only and C-N coupled models was done based on information provided in Table A.1 in (Friedlingstein et al., 2022).

S2 Meta-analysis of ecosystem experiments

S2.1 Statistical analysis

The natural logarithm of the response ratio of the means and its variance were calculated for each response variable, experiment, treatment, and sampling year, using information about the the number of repeated measurements (multiple experimental plots, multiple sampling dates per year). This was done using the function `escalc(measure="ROM", ...)` from the {metafor} R package (Viechtbauer, 2010). The standard error was calculated as $\text{SE} = \sqrt{\text{var}/N}$, where N is the number of repeated measurements.

For CO_2 experiments, the response ratio was normalised with (divided by) the natural logarithm of the ratio of elevated over ambient CO_2 concentrations.

Data was then aggregated by experiment using the procedure based on Borenstein (2009), implemented by the function `agg(method = "BHHR", ...)` from the {MAd} R package (Hoyt, 2014), and assuming a correlation of within-study response ratios of 0.5.

Finally, the meta-analysis of responses across experiments was performed as a mixed-effects meta-regression model using experiment as the grouping variable for random factors, and fitted via the restricted maximum likelihood esimation. This is implemented using the function `rma.mv(method = "REML", ...)` from the {metafor} R package (Viechtbauer, 2010). The confidence intervals (edges of boxes in Fig. 3) of the meta-analytic mean response ratio (bold line inside boxes in Fig. 3) span 95%.

S2.2 Response to CO2, MESI data

S2.2.1 Data selection

Data were used from the Manipulation Experiments Synthesis Initiative (MESI) database (Van Sundert et al., 2023), obtained from GitHub (`https://github.com/MESI-organization/mesi-db`). For CO_2 experiments, we considered only data from Free Air CO_2 Enrichment (FACE) experiments and from open-top chamber experiments, from experiments that provided data from at least three years. For data generated in multi-factorial experiments, we used only data from the CO_2-only treatment (no interactions with other experimentally manipulated factors considered). Variables shown in this manuscript (Fig. 3, 4, and 6 in this study) were identified by the response variable name in the database according to Tab. S1.

S2.2.2 Extended results

Table S1: Variables in the MESI database used for the analysis.

Variable name	Variable code	Variable names in MESI
AGB	agb	agb_coarse, agb
BGB	bgb	bgb, fine_root_biomass, coarse_root_c_stock, bgb_coarse
LAI	lai	lai, lai_max
Root NPP	root_production	root_production, fine_root_production, coarse_root_production
N uptake	n_uptake	root_n_uptake, root_nh4_uptake, root_no3_uptake
Inorganic N	n_inorg	soil_no3-n, soil_nh4-n, soil_nh4, soil_no3, soil_solution_nh4, soil_solution_no3
A_{sat}	asat	asat
V_{cmax}	vcmax	vcmax
J_{max}	jmax	jmax
GPP	gpp	gpp
N_{area}	leaf_n_area	leaf_n_area
N_{mass}	leaf_n_mass	leaf_n_mass
Leaf C:N	leaf_cn	leaf_cn
ANPP	anpp	anpp
Root:shoot	root_shoot_ratio	root_shoot_ratio

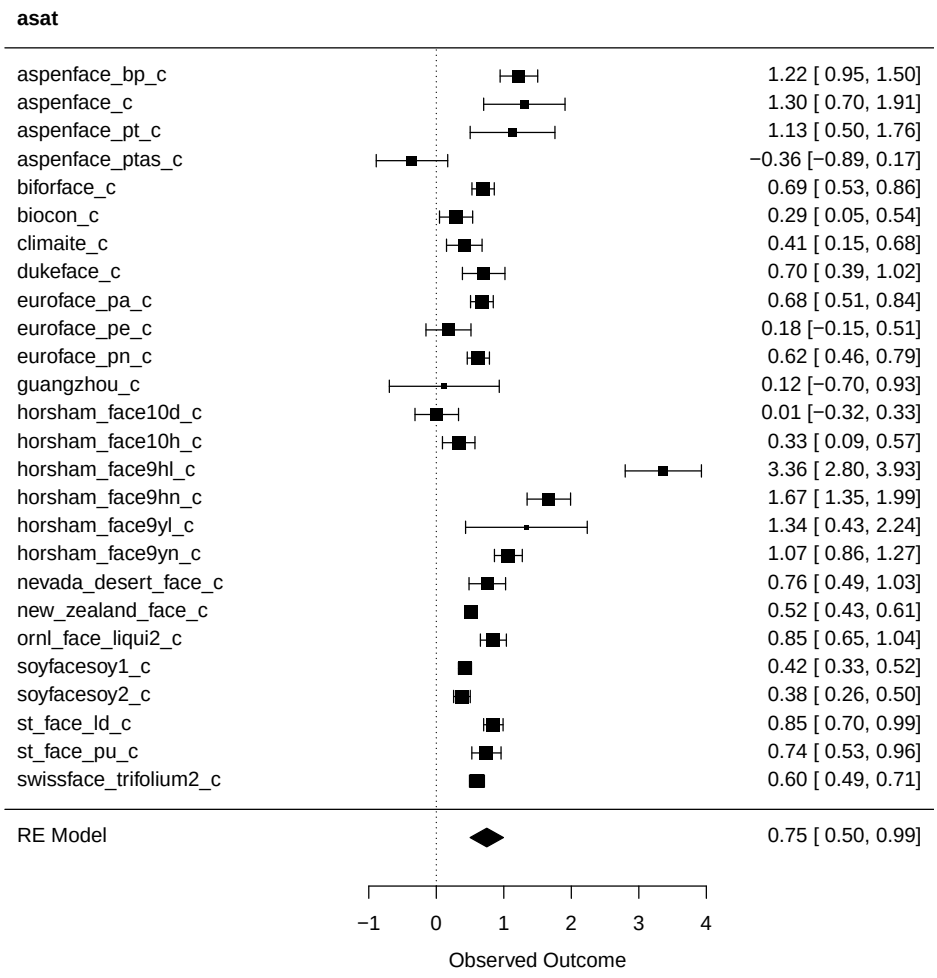

Figure S1: Response of leaf-level assimilation under light-saturated conditions (A_{sat}) to elevated CO_2 in individual experiments and meta-analytic mean across experiments. Plot created with `forest` from the {metafor} R package Viechtbauer (2010).

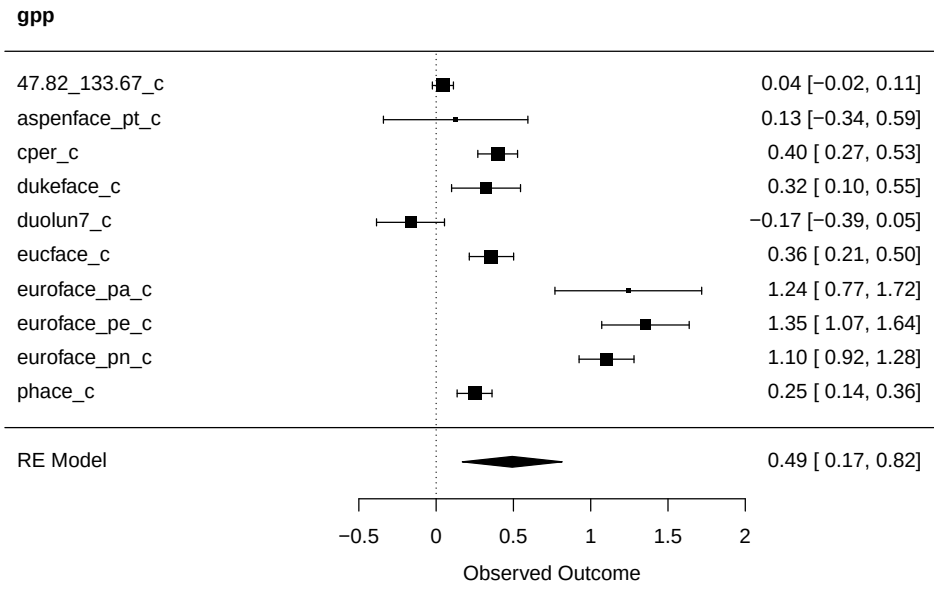

Figure S2: Response of GPP to elevated CO_2 in individual experiments and meta-analytic mean across experiments. Plot created with `forest` from the {metafor} R package Viechtbauer (2010).

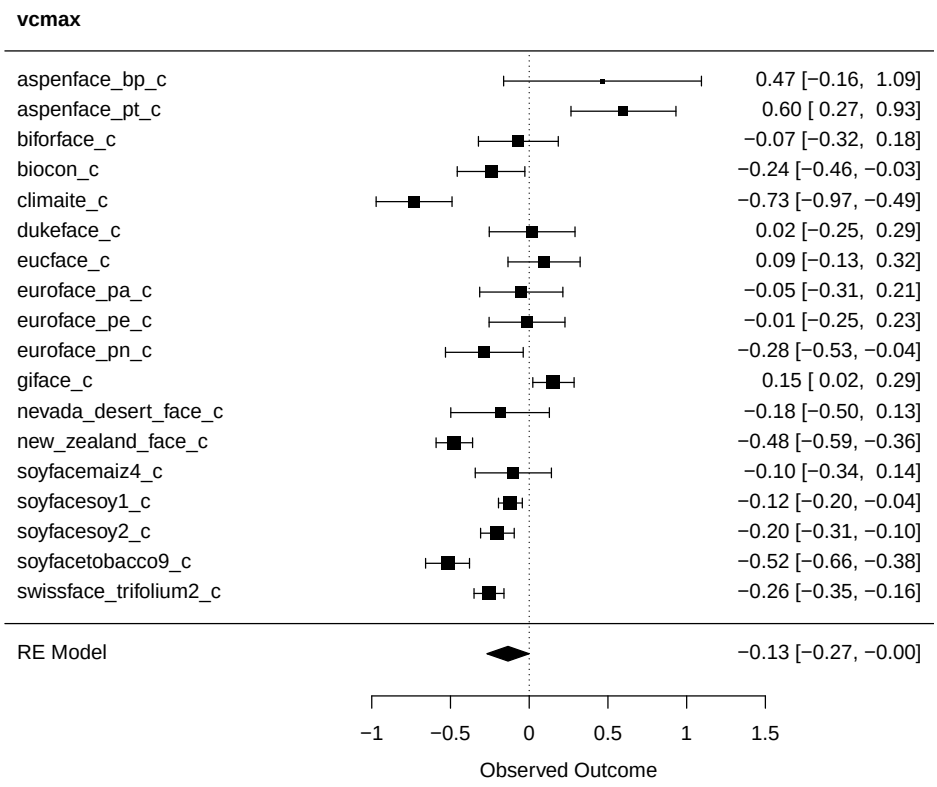

Figure S3: Response of V_{cmax} to elevated CO_2 in individual experiments and meta-analytic mean across experiments. Plot created with `forest` from the {metafor} R package Viechtbauer (2010).

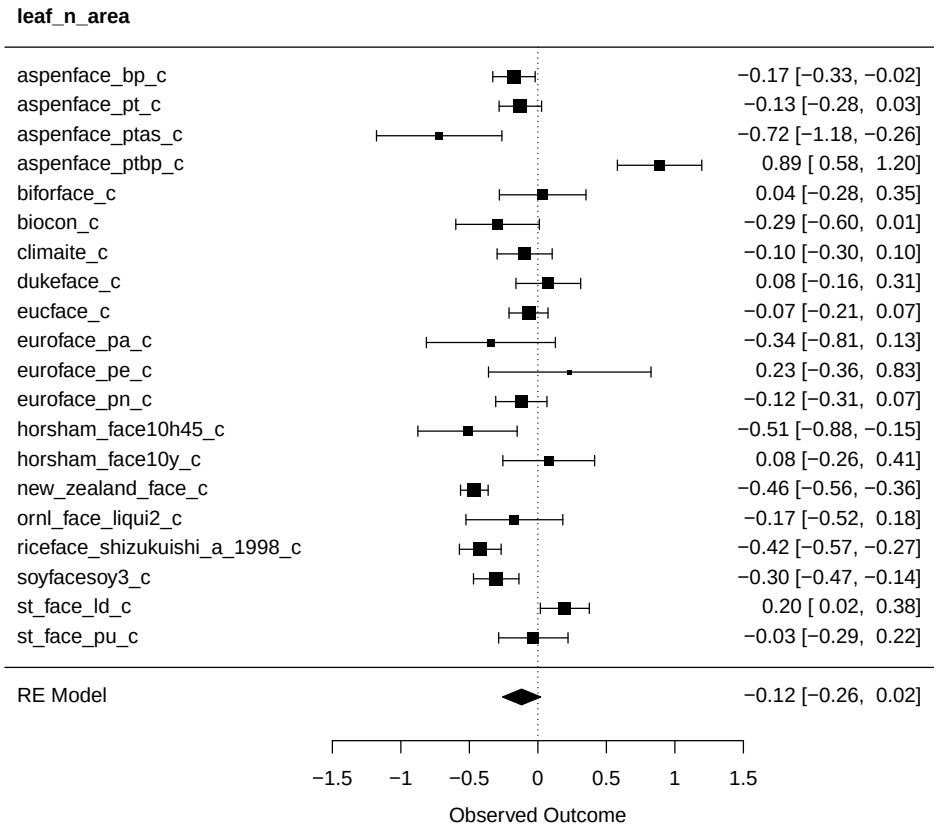

Figure S4: Response of leaf N_{area} to elevated CO_2 in individual experiments and meta-analytic mean across experiments. Plot created with `forest` from the {metafor} R package Viechtbauer (2010).

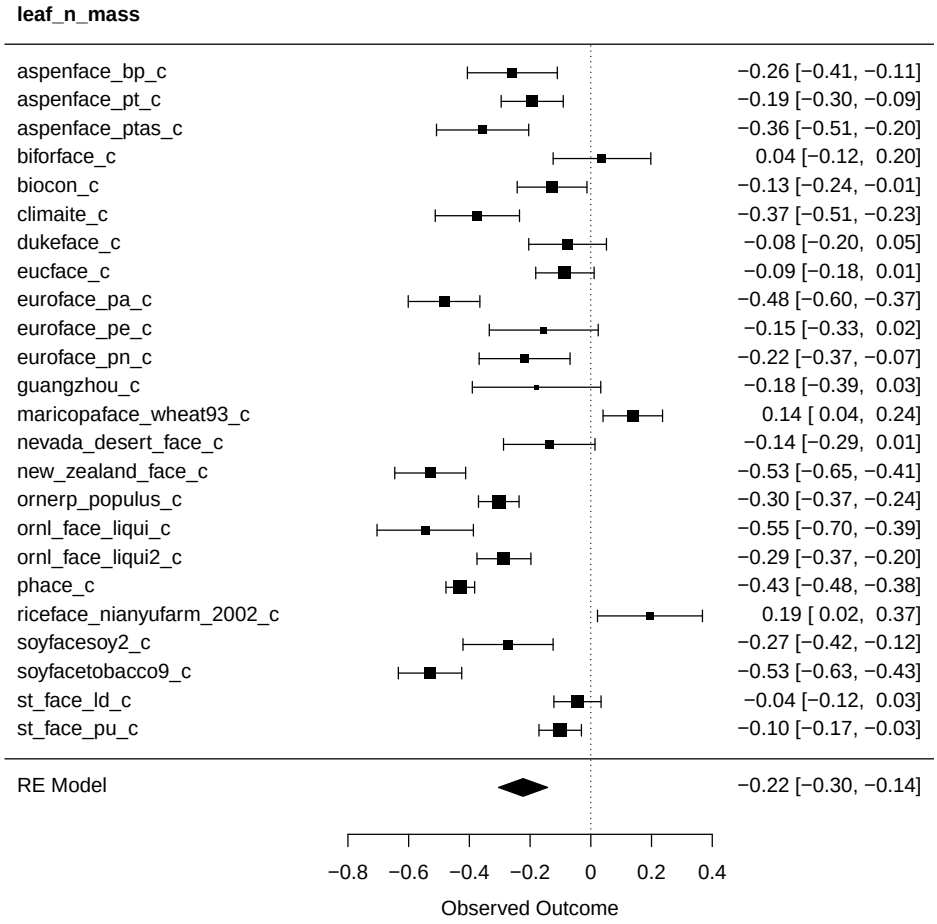

Figure S5: Response of leaf N_{mass} to elevated CO_2 in individual experiments and meta-analytic mean across experiments. Plot created with `forest` from the {metafor} R package Viechtbauer (2010).

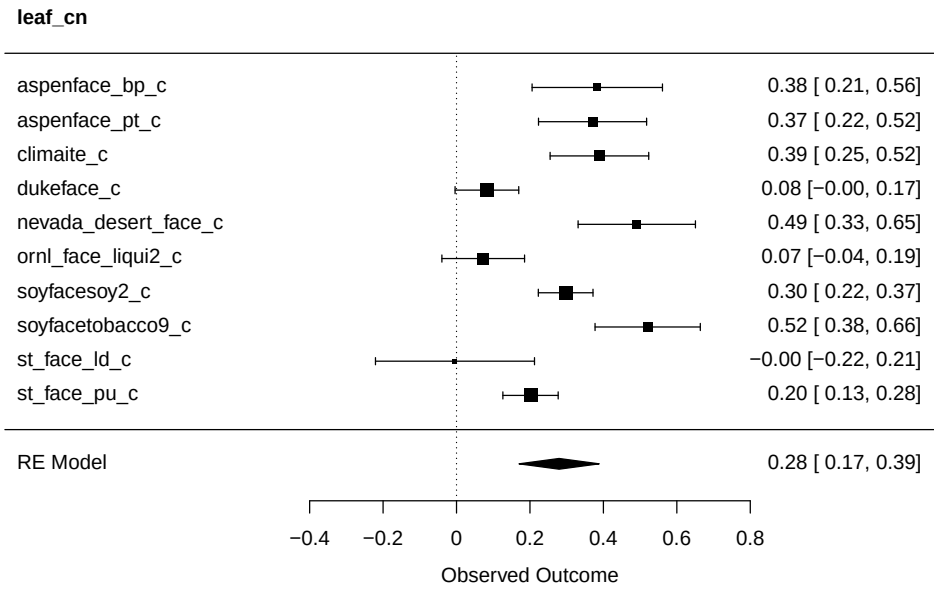

Figure S6: Response of leaf C:N to elevated CO_2 in individual experiments and meta-analytic mean across experiments. Plot created with `forest` from the {metafor} R package Viechtbauer (2010).

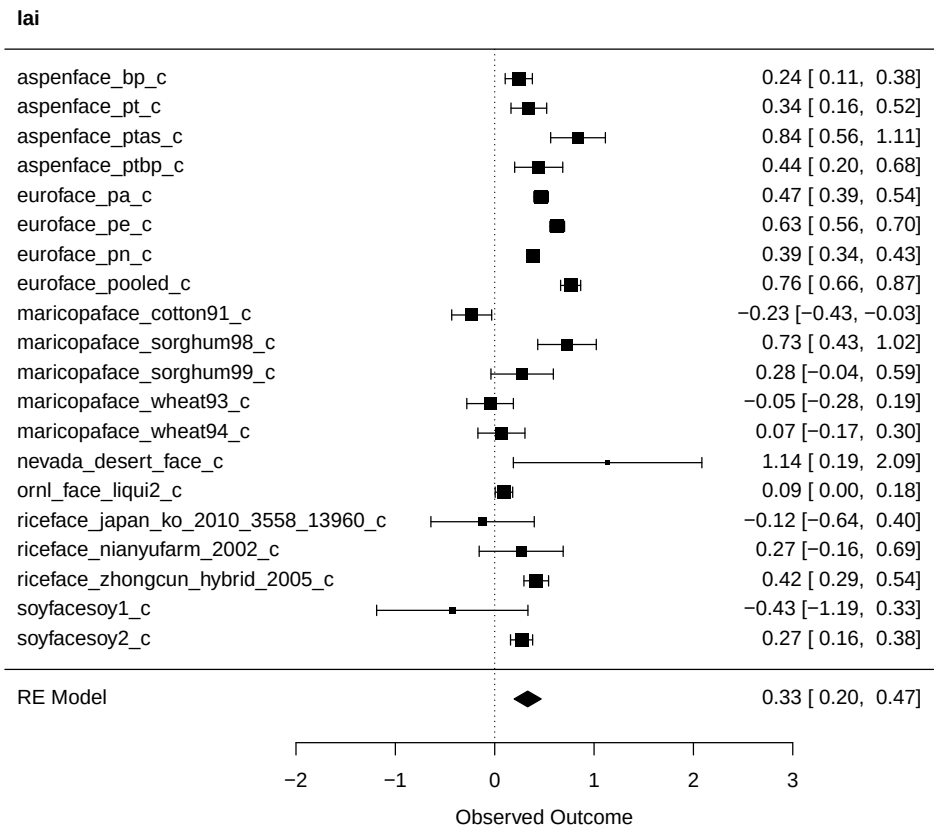

Figure S7: Response of LAI to elevated CO_2 in individual experiments and meta-analytic mean across experiments. Plot created with `forest` from the {metafor} R package Viechtbauer (2010).

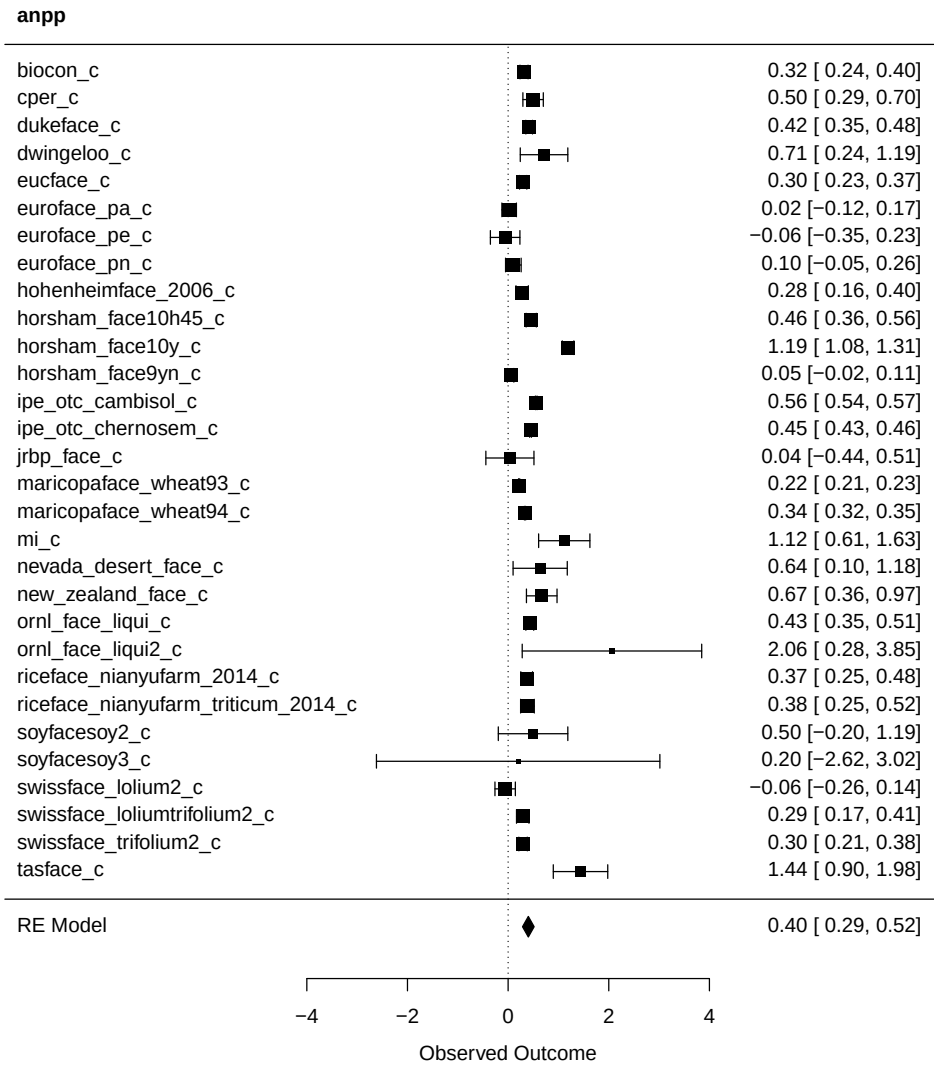

Figure S8: Response of aboveground net primary productivity (ANPP) to elevated CO_2 in individual experiments and meta-analytic mean across experiments. Plot created with `forest` from the {metafor} R package Viechtbauer (2010).

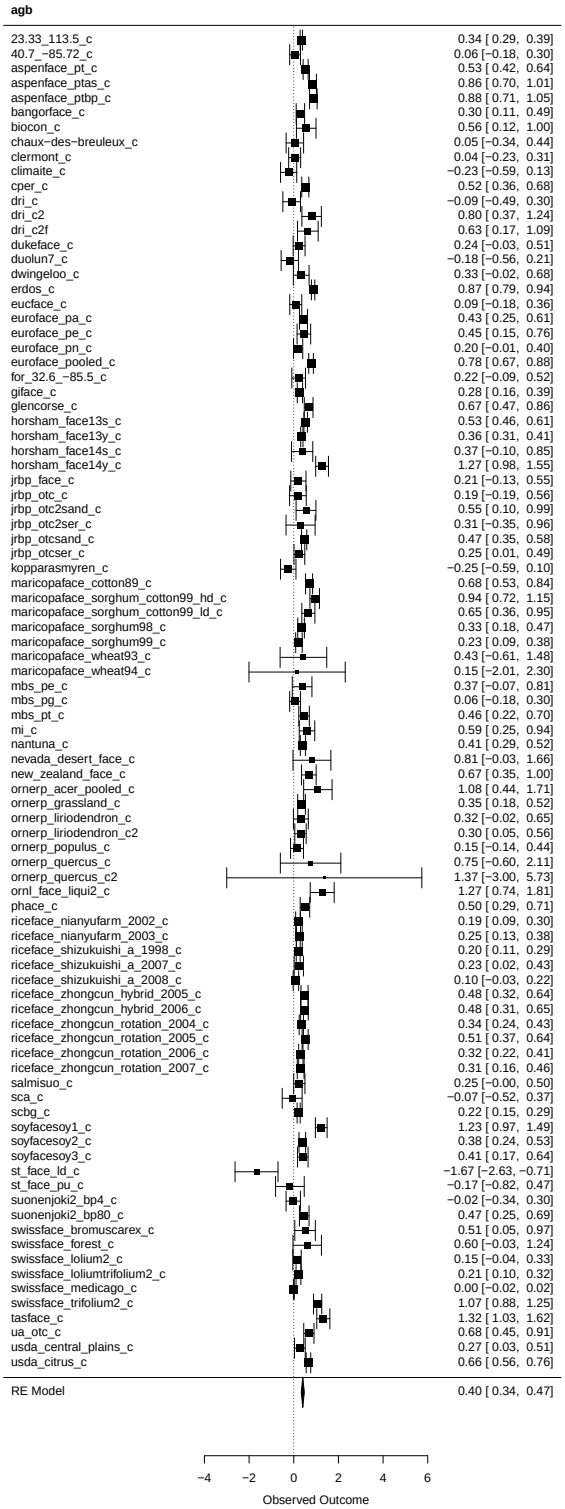

Figure S9: Response of aboveground biomass (AGB) to elevated CO_2 in individual experiments and meta-analytic mean across experiments. Plot created with `forest` from the {metafor} R package Viechtbauer (2010).

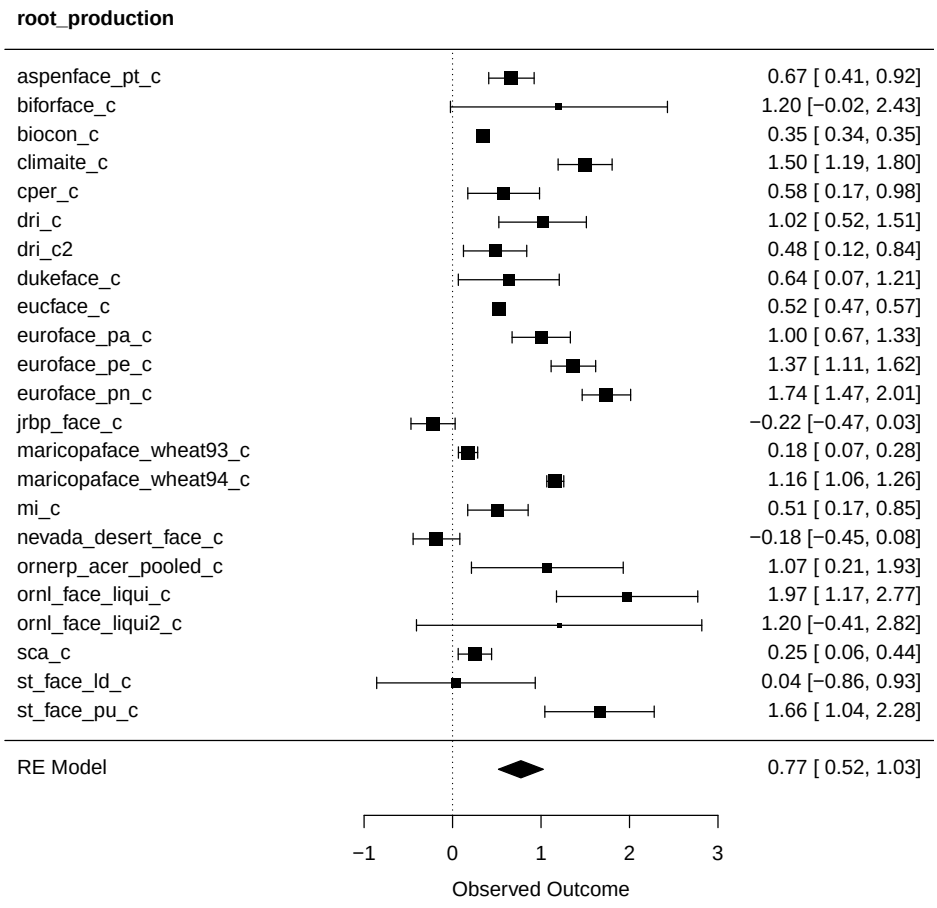

Figure S10: Response of root biomass productivity to elevated CO_2 in individual experiments and meta-analytic mean across experiments. Plot created with `forest` from the {metafor} R package Viechtbauer (2010).

S2.3 Response to N-fertilisation, MESI and NutNet data

S2.3.1 Data selection

Data were used from the Manipulation Experiments Synthesis Initiative (MESI) database (Van Sundert et al., 2023), obtained from GitHub (`https://github.com/MESI-organization/mesi-db`). For variables belowground biomass (bgb, `Rootsgperm2` in NutNet), root mass fraction (rmf, `rootmassfraction` in NutNet), aboveground biomass (agb), and the root:shoot ratio (root_shoot_ratio), we combined MESI data with data from the meta-analysis of the NutNet experiments network by Cleland et al. (2019). Aboveground biomass from NutNet data was calculated as (bgb/rmf) − bgb. The root:shoot ratio from NutNet data was calculated as bgb/agb.

For MESI data, only data from field experiments were used for which the N application rate was less or equal to 300 kg N ha^{-1} yr^{-1}. For data generated in multifactorial experiments, we used only data from the N-fertilisation-only treatment (no interactions with other experimentally manipulated factors considered). Variables shown in this manuscript (Fig. 3, 4, and 6 in this study) were identified by the response variable name in the database according to Tab. S1.

S2.3.2 Extended results

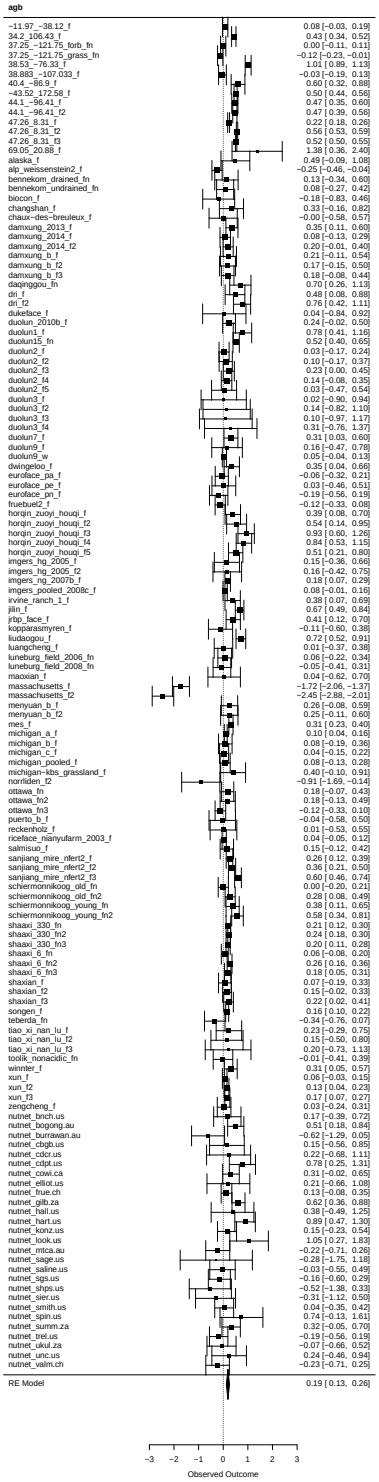

Figure S11: Response of aboveground biomass (agb) to N-fertilisation in individual experiments and meta-analytic mean across experiments. Plot created with `forest` from the {metafor} R package Viechtbauer (2010).

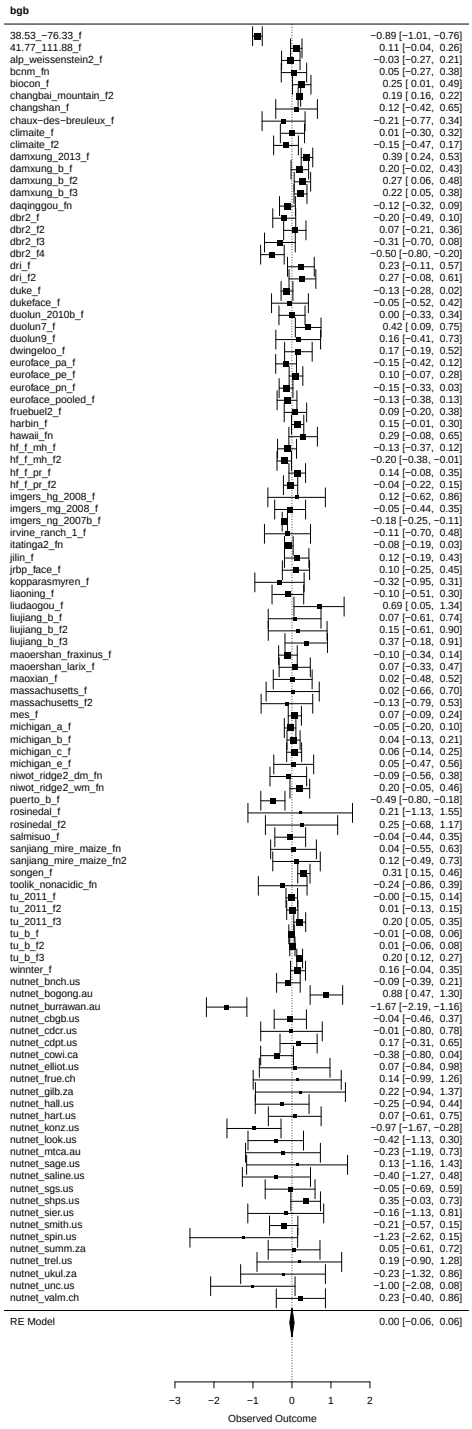

Figure S12: Response of belowground biomass (bgb) to N-fertilisation in individual experiments and meta-analytic mean across experiments. Plot created with `forest` from the {metafor} R package Viechtbauer (2010).

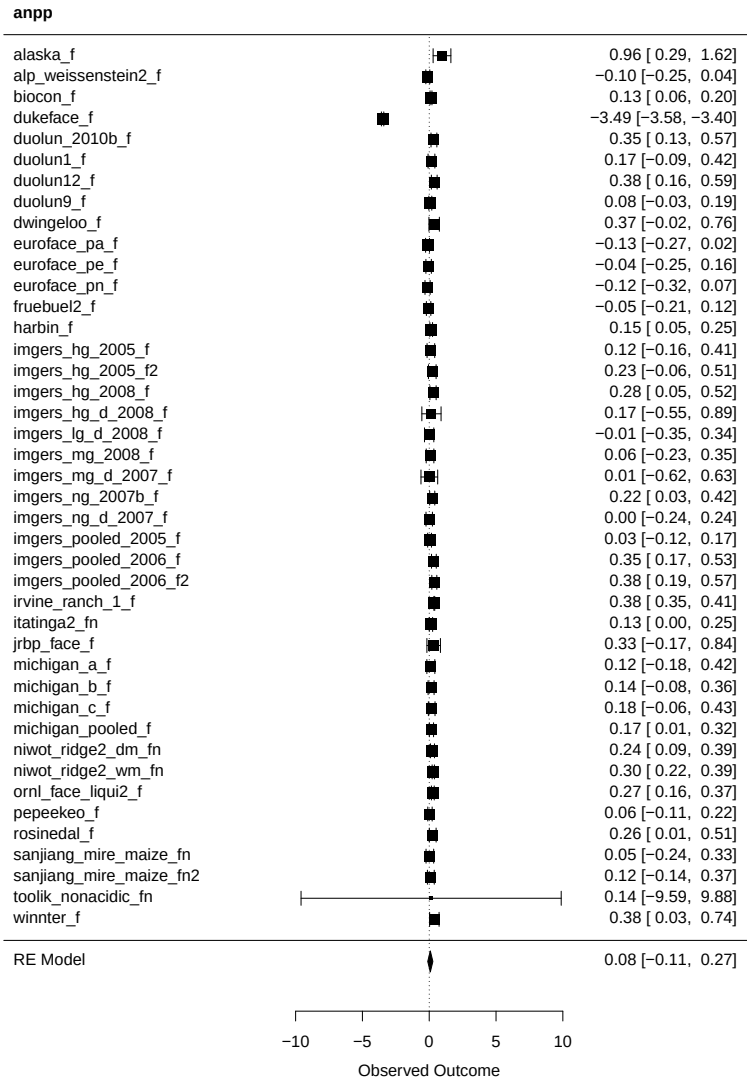

Figure S13: Response of aboveground net primariy production (anpp) to N-fertilisation in individual experiments and meta-analytic mean across experiments. Plot created with `forest` from the {metafor} R package Viechtbauer (2010).

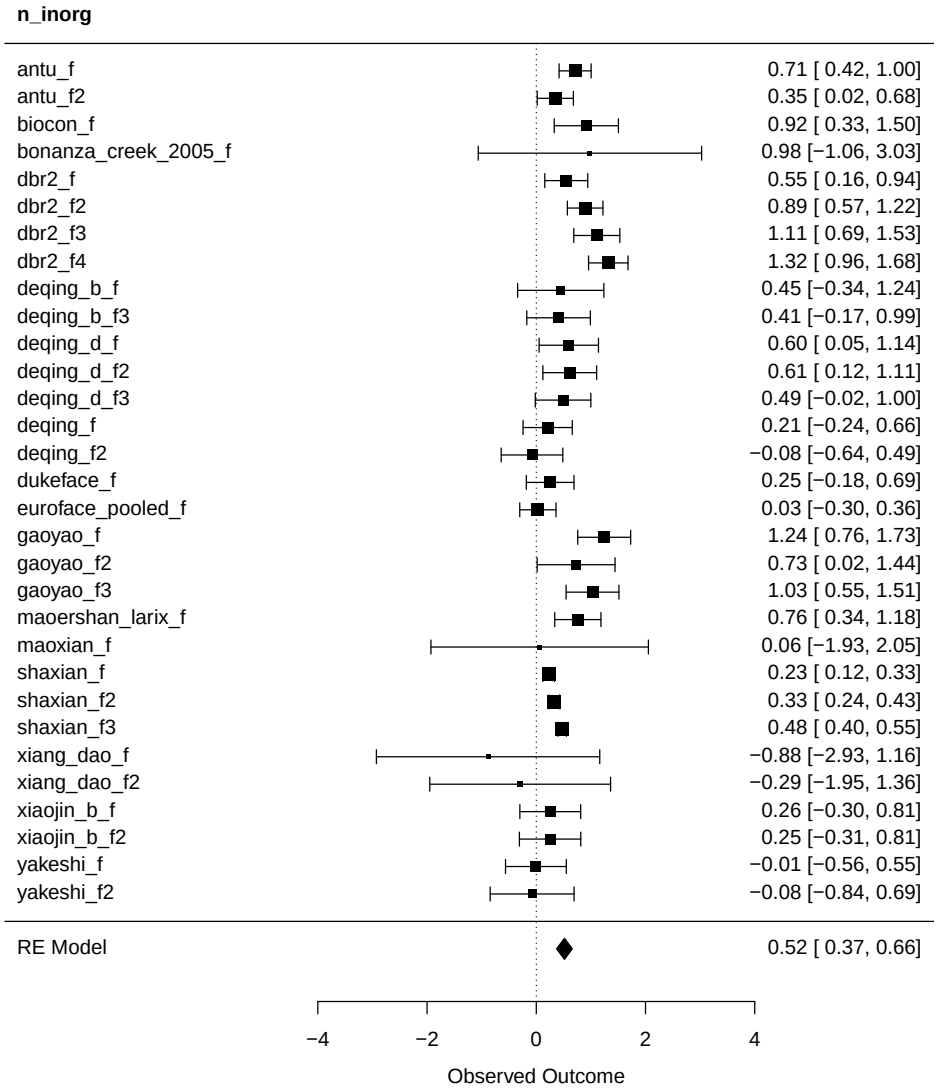

Figure S14: Response of soil inorganic nitrogen (n_inorg) to N-fertilisation in individual experiments and meta-analytic mean across experiments. Plot created with `forest` from the {metafor} R package Viechtbauer (2010).

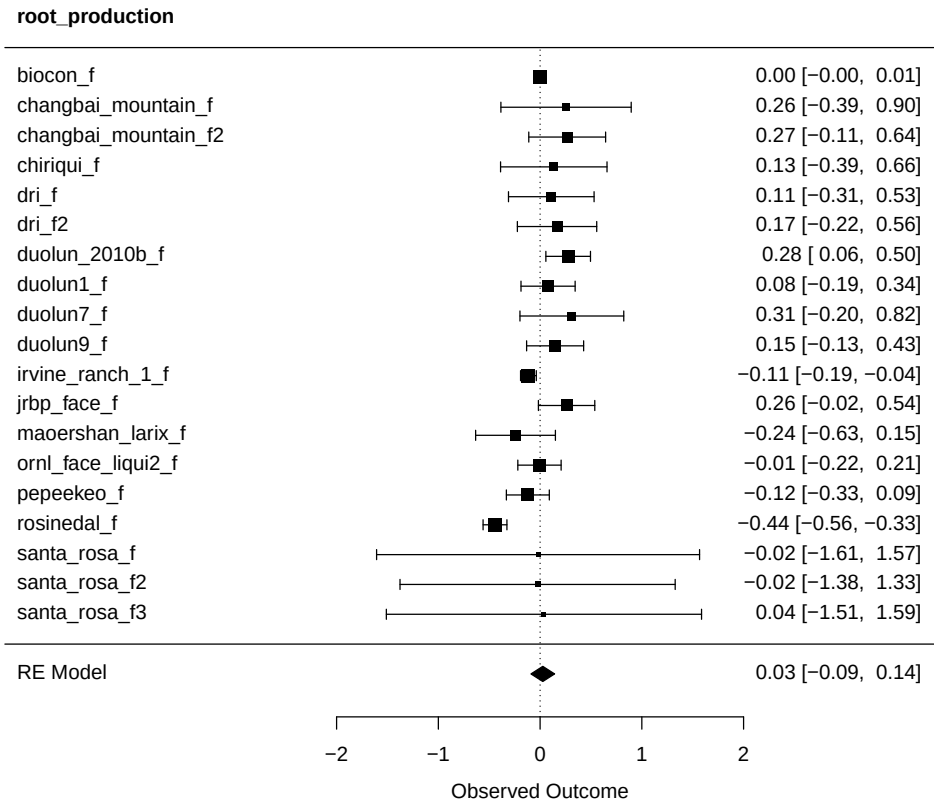

Figure S15: Response of root biomass production (root_production) to N-fertilisation in individual experiments and meta-analytic mean across experiments. Plot created with `forest` from the {metafor} R package Viechtbauer (2010).

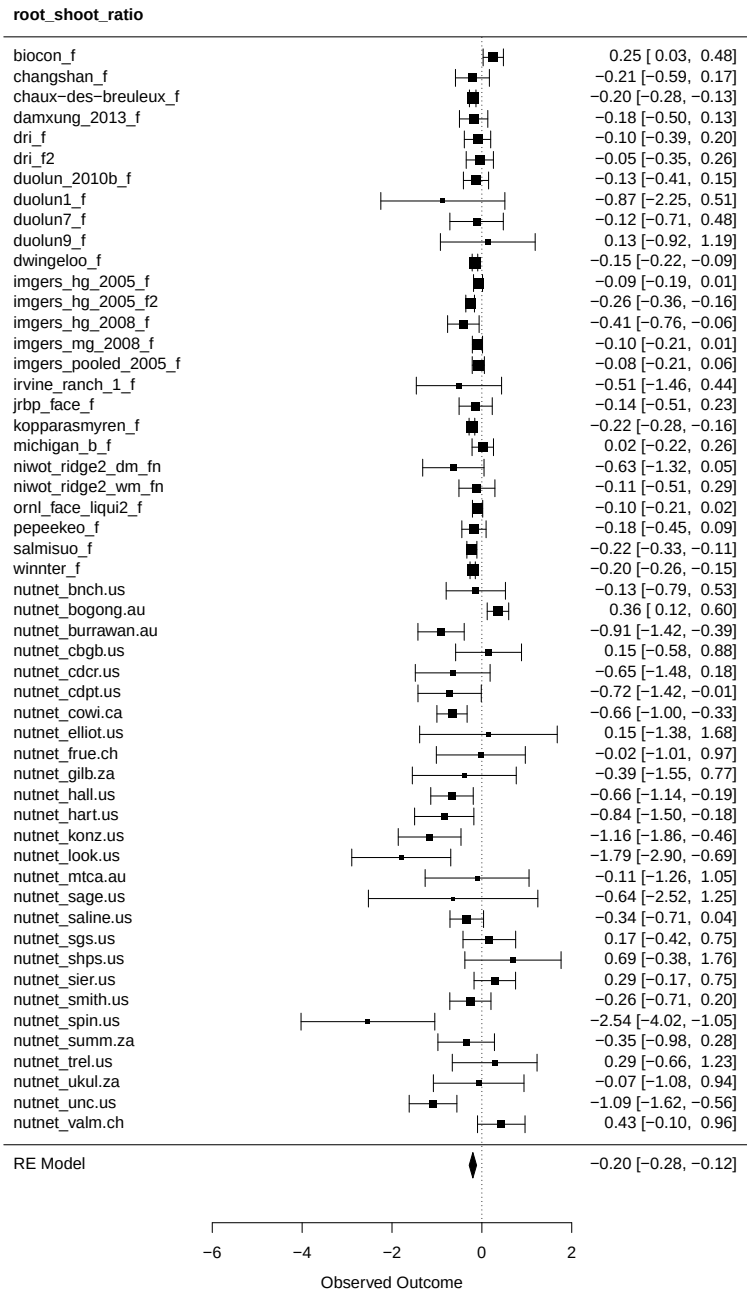

Figure S16: Response of the root:shoot ratio (root_shoot_ratio) to N-fertilisation in individual experiments and meta-analytic mean across experiments. Plot created with `forest` from the {metafor} R package Viechtbauer (2010).

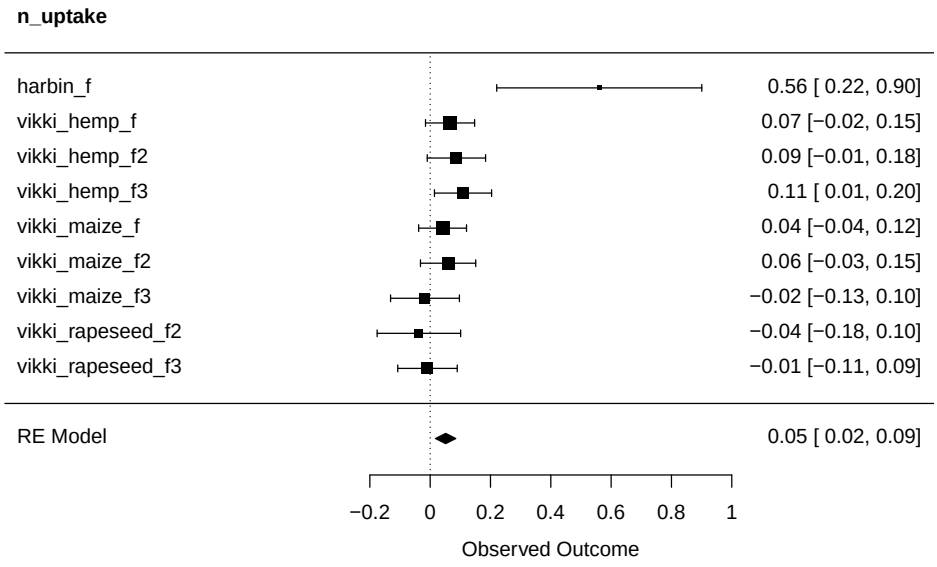

Figure S17: Response of the N uptake ratio (n_uptake) to N-fertilisation in individual experiments and meta-analytic mean across experiments. Plot created with `forest` from the {metafor} R package Viechtbauer (2010).

S2.4 Response to N-fertilisation, Liang et al. data

S2.4.1 Data selection

Data were used from the meta-analysis by Liang et al. (2020) for which the N application rate was less or equal to 300 kg N ha^{-1} yr^{-1}.

S2.4.2 Extended results

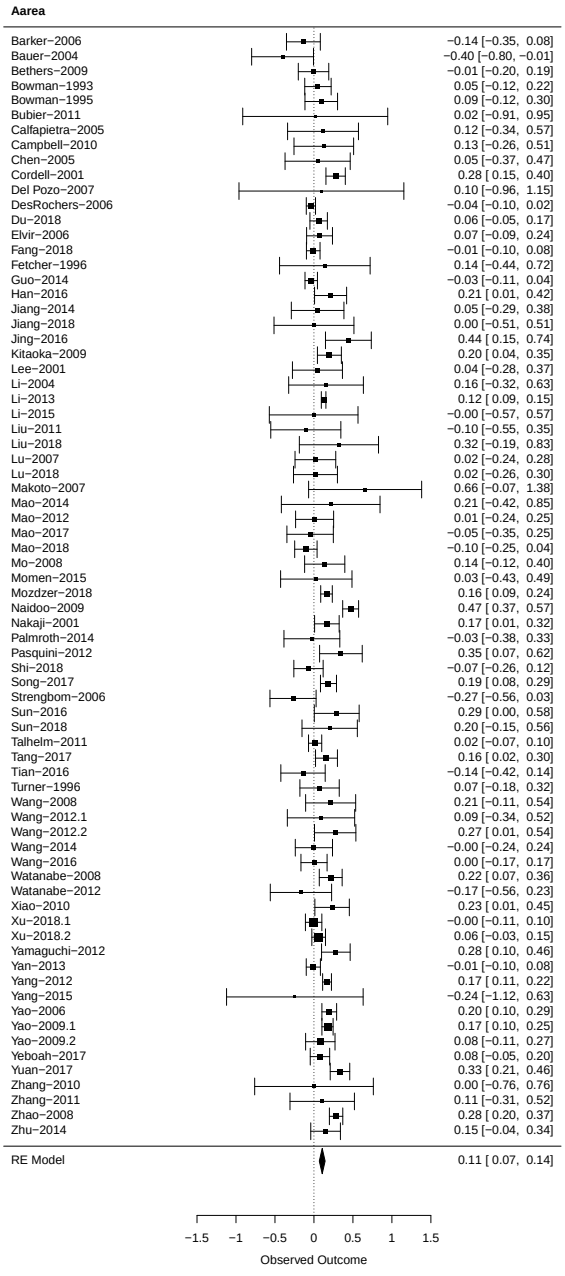

Figure S18: Response of leaf-level assimilation rate (Aarea), here interpreted as representative for light-saturated conditions, to N-fertilisation in individual experiments and meta-analytic mean across experiments. Plot created with `forest` from the {metafor} R package Viechtbauer (2010).

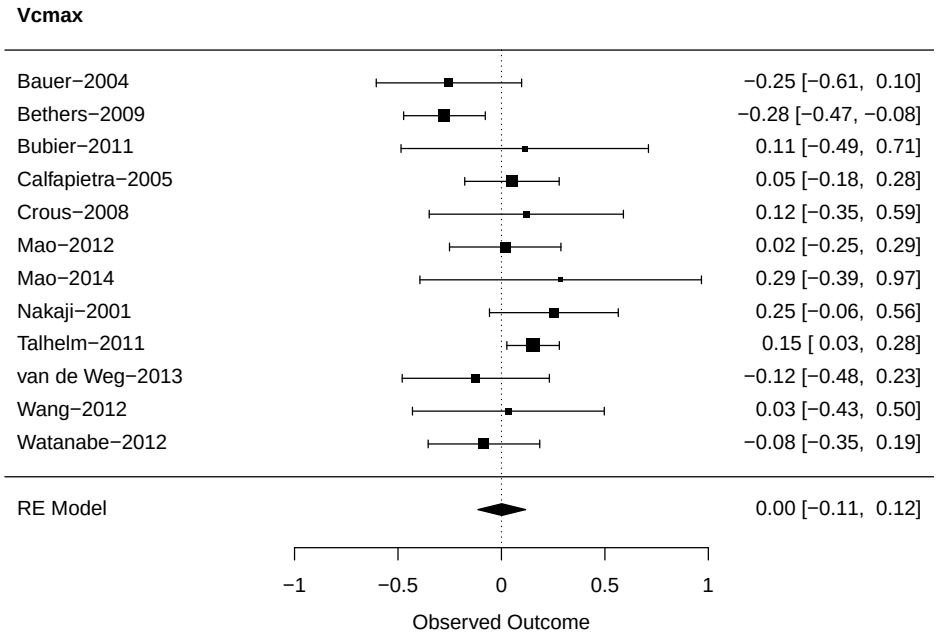

Figure S19: Response of V_{cmax} to N-fertilisation in individual experiments and meta-analytic mean across experiments. Plot created with `forest` from the {metafor} R package Viechtbauer (2010).

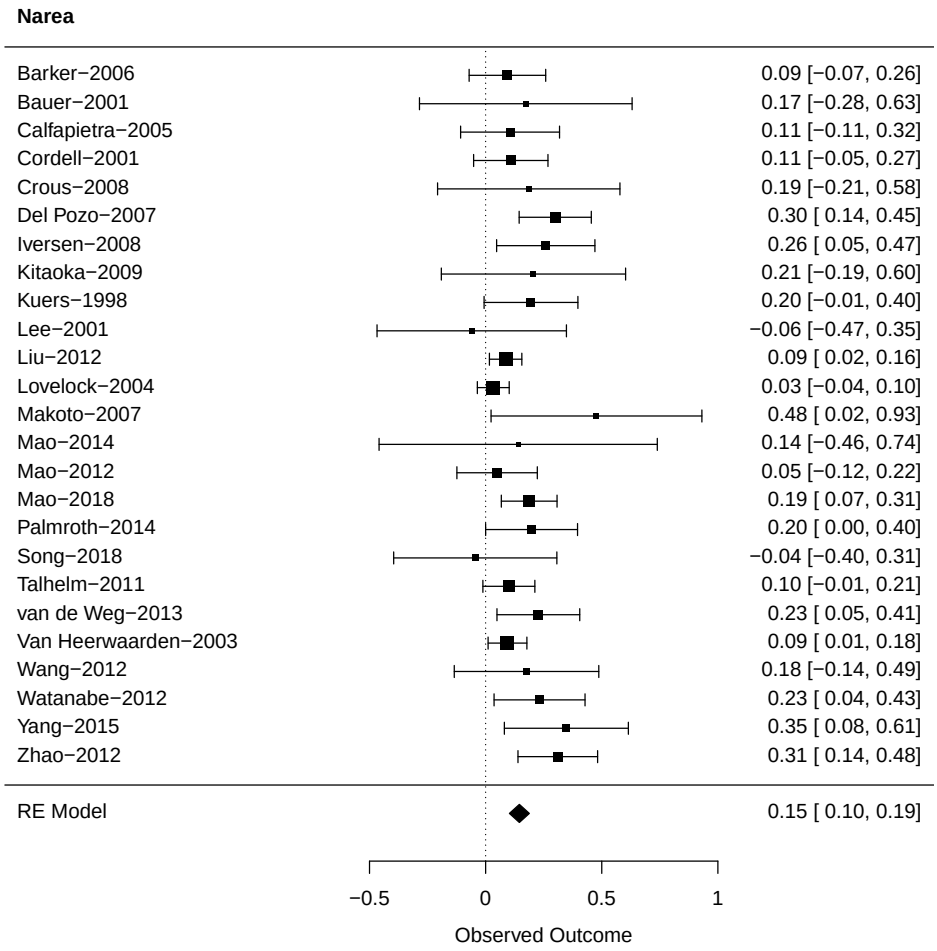

Figure S20: Response of N_{area} (Narea) to N-fertilisation in individual experiments and meta-analytic mean across experiments. Plot created with `forest` from the {metafor} R package Viechtbauer (2010).

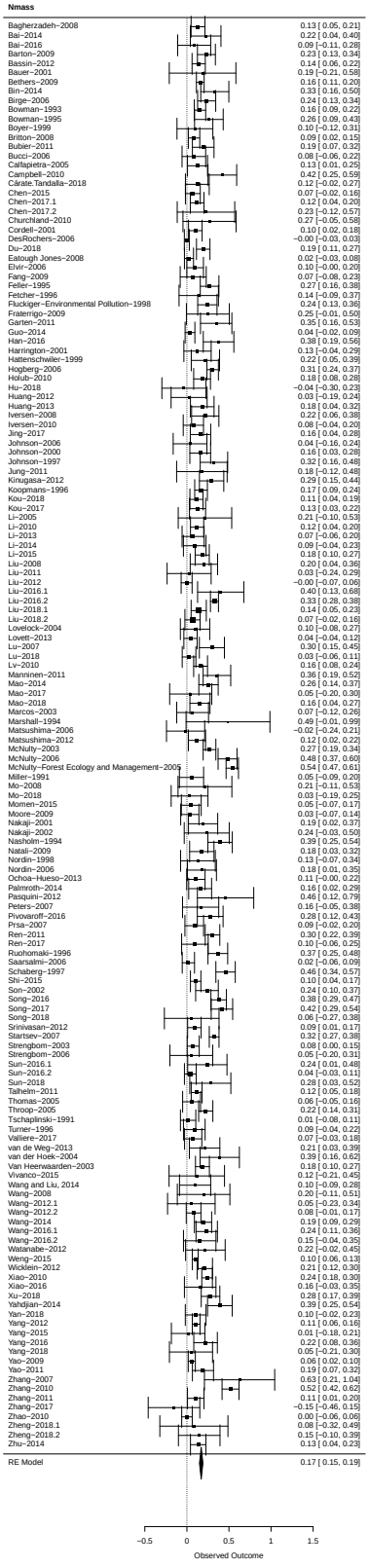

Figure S21: Response of N_{mass} (Nmass) to N-fertilisation in individual experiments and meta-analytic mean across experiments. Plot created with `forest` from the {metafor} R package Viechtbauer (2010).

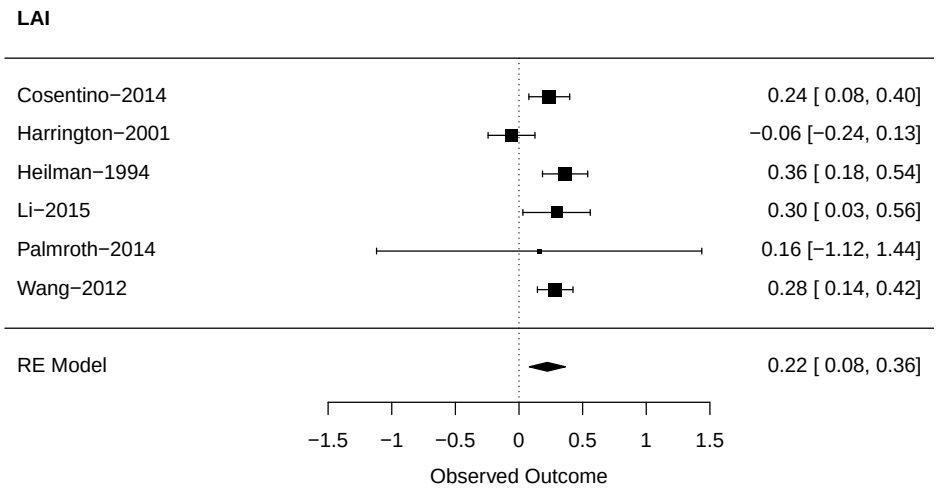

Figure S22: Response of the leaf area index (LAI) to N-fertilisation in individual experiments and meta-analytic mean across experiments. Plot created with `forest` from the {metafor} R package Viechtbauer (2010).

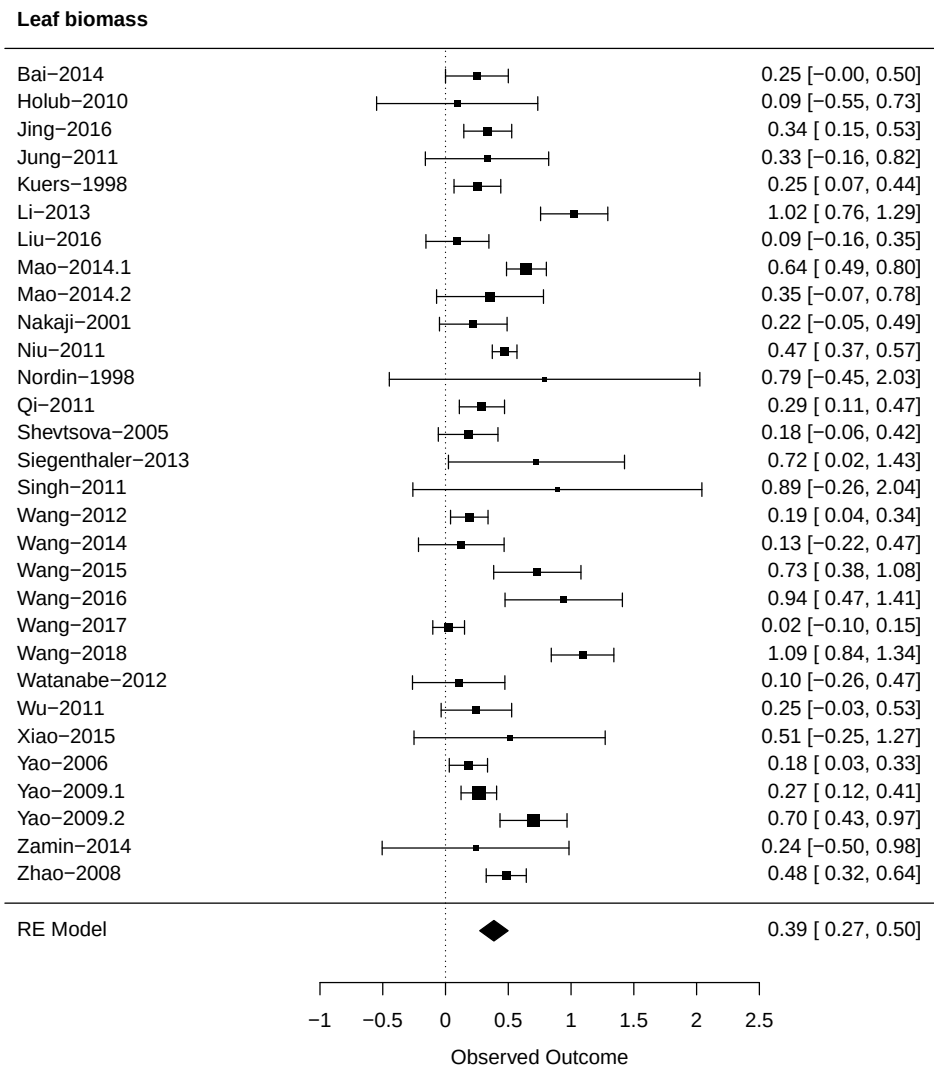

Figure S23: Response of leaf biomass to N-fertilisation in individual experiments and meta-analytic mean across experiments. Plot created with `forest` from the {metafor} R package Viechtbauer (2010).

S3 Analysis of global leaf traits data

The analysis was based on data from Dong et al. (2022b), obtained through Zenodo (Dong et al., 2022a). The data contains 3143 observations from 2078 different plant species, collected at 302 different sites where plants were growing under natural conditions (not experimentally disturbed). The target variables of the analysis are leaf N content per unit leaf area (N_{area}, leaf N content per unit leaf mass (N_{mass}, leaf dry mass perunit leaf area (LMA), and the Rubisco carboxylation capacity at the standard temperature of 25°C - a measure of the capacity of photosynthesis under non-light limiting conditions and linked with the leaf metabolic N content through the N-richness of Rubisco. All target variables were log-transformed to improve normality of the model residuals.

Soil C:N ratio was extracted from ISRIC WISE30sec (Batjes, 2016). Growth temperature (T_{growth}) was derived from the monthly climatology of WorldClim extracted from global 1 km resolution maps (Fick and Hijmans, 2017) and calculated as the daytime mean temperature (conversion of mean daily to daytime mean temperature following Jones (2013), see Eq. 9 in Dong et al. (2022b)) of months for which the daytime temperature was > 0°C. The photosynthetic photon flux density (PPFD) was calculated as a linear function of shorwave incoming radiation. Vapour pressure deficit (VPD) was calculated from monthly climatologies of vapour pressure, daily minimum and maximum temperature from WorldClim as

$$\text{VPD} = \left(\text{VPD}(e_a, T_{\text{min}}) + \text{VPD}(e_a, T_{\text{max}})\right)/2 \ , \tag{S2}$$

with

$$\text{VPD}(e_a, T) = e_s - e_a \ , \tag{S3}$$

where e_a is the actual vapour pressure, obtained from WorldClim. and e_s is the saturation vapour pressure, calculated as

$$e_s = 611.0 \ \exp\left(\frac{17.27\, T}{T + 237.3}\right) \ . \tag{S4}$$

Also VPD and PPFD were averaged over months with mean growth temperatures above freezing from the monthly WorldClim climatology to obtain a growing-season mean.

Nitrogen deposition was taken from Lamarque et al. (2011) as the sum of atmospheric deposition of NH_x and NO_y and averaged over years 1990 to 2009. N deposition and VPD were log-transformed for further analysis since their distributions were highly asymmetric.

Ordinary least-squares linear regression models were fitted separately for each target variable with the same centered and scaled predictors. Centering and scaling enables the quantitative comparison of fitted coefficients as a measure of variable importance and partial effect magnitude. Variance inflation factors were below five for all variables. Values for the 'normalised slope' shown in Fig. 5 of the main text are taken as the coefficients of the five predictors determined from the fitted linear regression models of each target variable.

A summary of the models, including coefficients and goodness-of-fit metrics, is given in Table S2.

Table S2: Summaries for linear regression models of leaf traits and environmental predictors. Coefficients of the five scaled predictors are shown along rows for the different target variables along columns. Values of the coefficients correspond to the values shown in Fig. 5 of the main text. The standard error of coefficient estimates is given in brackets. Asterisks indicate significance of each predictor at different levels (see table note). The number of observations (*N*) and goodness-of-fit metrics are given in the bottom three rows of the table. N dep. is nitrogen deposition.

	V_{cmax}	N_{area}	N_{mass}	LMA
VPD	0.201^{***}	0.226^{***}	-0.094^{***}	0.320^{***}
	(0.017)	(0.014)	(0.012)	(0.017)
PPFD	0.062^{***}	$-0.020+$	0.038^{***}	-0.057^{***}
	(0.013)	(0.011)	(0.009)	(0.012)
T_{growth}	-0.270^{***}	-0.159^{***}	0.096^{***}	-0.255^{***}
	(0.016)	(0.014)	(0.012)	(0.016)
Soil C:N	-0.044^{***}	-0.066^{***}	-0.075^{***}	0.009
	(0.010)	(0.008)	(0.007)	(0.010)
N dep.	-0.006	-0.131^{***}	0.127^{***}	-0.257^{***}
	(0.012)	(0.010)	(0.009)	(0.012)
N	3137	3134	3134	3134
R^2	0.111	0.154	0.097	0.209
Adj. R^2	0.109	0.152	0.095	0.208

+ $p < 0.1$, * $p < 0.05$, ** $p < 0.01$, *** $p < 0.001$

S4 CN-model simulations

The CN-model is used here for two point-scale simulations - one with a step-increase to elevated CO_2 and one with a step-increase in reactive N input. For both simulations, the daily meteorological forcing time series are derived from FLUXNET2015 data for the site FR-Pue (Rambal et al., 2004) - the site of an evergreen forest in southern France. For the demonstration purpose of the simulations here, we forced the model with constant meteorological conditions in each day and simulation year. Constant meteorological conditions were taken as growing-season mean, i.e., the average over all days where air temperature was above 5°C. Effects of limiting root-zone water availability are not considered for the CN-model simulations.

The ambient daily N deposition is set to 0.003 gN m^{-2} d^{-1}. These values are chosed such that the annual sum of NO_3 and NH_4 correspond to values for this site location estimated by global atmospheric chemitry and transport modelling (Lamarque et al., 2011).

No biomass harvesting, nor external seed input was considered.

For the CO_2 experiment, the atmospheric concentration was doubled, from 389 ppm to 778 ppm, within one year. The simulated and observed responses to elevated CO_2 were normalised with the change in CO_2 (see S2.1) for the evaluation against observations from the experiments meta-analysis. For the N-fertilisation experiment, the reactive N input was increased from the ambient level to 12 gN m^{-2} d^{-1}. This corresponds to the average rate of fertilisation experiments in (Liang et al., 2020). Simulated response ratios were evaluated as means across ten years (year 5 to 15) after the step-increase, and referenced against three years before the step-increase. The first four years after the step-increase were omitted because of oscillating behaviour of the modelled system, which got attenuated thereafter.

Model simulations were performed with the model as implemented in the rsofun modelling framework available from `https://github.com/stineb/rsofun/tree/cnmodel` branch `cnmodel`, commit hash number `66b424142b500e07c41895dbb35d64e5bbdad49e`). Model parameters are specified in the scripts available on Github (`https://github.com/stineb/lt_cn_review/blob/main/analysis/exp_co2_cnmodel.R` and `https://github.com/stineb/lt_cn_review/blob/main/analysis/exp_nfert_cnmodel.R`).

References

Batjes, N. H.: Harmonized soil property values for broad-scale modelling (WISE30sec) with estimates of global soil carbon stocks, Geoderma, 269, 61–68, https://doi.org/10.1016/j.geoderma.2016.01.034, URL https://www.sciencedirect.com/science/article/pii/S0016706116300349, 2016.

Borenstein, M.: Effect sizes for continuous data, in: The handbook of research synthesis and meta-analysis, 2nd ed, pp. 221–235, Russell Sage Foundation, New York, NY, US, 2009.

Cleland, E. E., Lind, E. M., DeCrappeo, N. M., DeLorenze, E., Wilkins, R. A., Adler, P. B., Bakker, J. D., Brown, C. S., Davies, K. F., Esch, E., Firn, J., Gressard, S., Gruner, D. S., Hagenah, N., Harpole, W. S., Hautier, Y., Hobbie, S. E., Hofmockel, K. S., Kirkman, K., Knops, J., Kopp, C. W., La Pierre, K. J., MacDougall, A., McCulley, R. L., Melbourne, B. A., Moore, J. L., Prober, S. M., Riggs, C., Risch, A. C., Schuetz, M., Stevens, C., Wragg, P. D., Wright, J., Borer, E. T., and Seabloom, E. W.: Belowground Biomass Response to Nutrient Enrichment Depends on Light Limitation Across Globally Distributed Grasslands, Ecosystems, 22, 1466–1477, https://doi.org/10.1007/s10021-019-00350-4, URL https://doi.org/10.1007/s10021-019-00350-4, 2019.

Dong, N., Prentice, I. C., Wright, I., Wang, H., Atkin, O., Bloomfield, K., Domingues, T., Gleason, S., Maire, V., Onoda, Y., Poorter, H., and Smith, N.: dataset for paper "Leaf nitrogen from the perspective of optimal plant function", https://doi.org/10.5281/zenodo.6831903, URL https://doi.org/10.5281/zenodo.6831903, 2022a.

Dong, N., Prentice, I. C., Wright, I. J., Wang, H., Atkin, O. K., Bloomfield, K. J., Domingues, T. F., Gleason, S. M., Maire, V., Onoda, Y., Poorter, H., and Smith, N. G.: Leaf nitrogen from the perspective of optimal plant function, Journal of Ecology, 110, 2585–2602, https://doi.org/10.1111/1365-2745.13967, URL https://besjournals.onlinelibrary.wiley.com/doi/10.1111/1365-2745.13967, 2022b.

Fick, S. E. and Hijmans, R. J.: WorldClim 2: new 1-km spatial resolution climate surfaces for global land areas, International Journal of Climatology, 37, 4302–4315, https://doi.org/10.1002/joc.5086, URL https://onlinelibrary.wiley.com/doi/abs/10.1002/joc.5086, _eprint: https://onlinelibrary.wiley.com/doi/pdf/10.1002/joc.5086, 2017.

Friedlingstein, P., Jones, M. W., O'Sullivan, M., Andrew, R. M., Bakker, D. C. E., Hauck, J., Le Quéré, C., Peters, G. P., Peters, W., Pongratz, J., Sitch, S., Canadell, J. G., Ciais, P., Jackson, R. B., Alin, S. R., Anthoni, P., Bates, N. R., Becker, M., Bellouin, N., Bopp, L., Chau, T. T. T., Chevallier, F., Chini, L. P., Cronin, M., Currie, K. I., Decharme, B., Djeutchouang, L. M., Dou, X., Evans, W., Feely, R. A., Feng, L., Gasser, T., Gilfillan, D., Gkritzalis, T., Grassi, G., Gregor, L., Gruber, N., Gürses, O., Harris, I., Houghton, R. A., Hurtt, G. C., Iida, Y., Ilyina, T., Luijkx, I. T., Jain, A., Jones, S. D., Kato, E., Kennedy, D., Klein Goldewijk, K., Knauer, J., Korsbakken, J. I., Körtzinger, A., Landschützer, P., Lauvset, S. K., Lefèvre, N., Lienert, S., Liu, J., Marland, G., McGuire, P. C., Melton, J. R., Munro, D. R., Nabel, J. E. M. S., Nakaoka, S.-I., Niwa, Y., Ono, T., Pierrot, D., Poulter, B.,

Rehder, G., Resplandy, L., Robertson, E., Rödenbeck, C., Rosan, T. M., Schwinger, J., Schwingshackl, C., Séférian, R., Sutton, A. J., Sweeney, C., Tanhua, T., Tans, P. P., Tian, H., Tilbrook, B., Tubiello, F., van der Werf, G. R., Vuichard, N., Wada, C., Wanninkhof, R., Watson, A. J., Willis, D., Wiltshire, A. J., Yuan, W., Yue, C., Yue, X., Zaehle, S., and Zeng, J.: Global Carbon Budget 2021, Earth System Science Data, 14, 1917–2005, https://doi.org/10.5194/essd-14-1917-2022, URL `https://essd.copernicus.org/articles/14/1917/2022/`, 2022.

Hoyt, A. C. D. R. . W. T.: MAd: Meta-Analysis with Mean Differences, URL `https://CRAN.R-project.org/package=MAd`, 2014.

Jones, H. G.: Plants and Microclimate: A Quantitative Approach to Environmental Plant Physiology, Cambridge University Press, Cambridge, 3 edn., https://doi.org/10.1017/CBO9780511845727, URL `https://www.cambridge.org/core/books/plants-and-microclimate/A7420295742E44198D8984F21D921058`, 2013.

Lamarque, J.-F., Kyle, G. P., Meinshausen, M., Riahi, K., Smith, S. J., van Vuuren, D. P., Conley, A. J., and Vitt, F.: Global and regional evolution of short-lived radiatively-active gases and aerosols in the Representative Concentration Pathways, Climatic Change, 109, 191, https://doi.org/10.1007/s10584-011-0155-0, URL `https://doi.org/10.1007/s10584-011-0155-0`, 2011.

Liang, X., Zhang, T., Lu, X., Ellsworth, D. S., BassiriRad, H., You, C., Wang, D., He, P., Deng, Q., Liu, H., Mo, J., and Ye, Q.: Global response patterns of plant photosynthesis to nitrogen addition: A meta-analysis, Global Change Biology, 26, 3585–3600, https://doi.org/10.1111/gcb.15071, URL `https://onlinelibrary.wiley.com/doi/abs/10.1111/gcb.15071`, _eprint: https://onlinelibrary.wiley.com/doi/pdf/10.1111/gcb.15071, 2020.

Rambal, S., Joffre, R., Ourcival, J. M., Cavender-Bares, J., and Rocheteau, A.: The growth respiration component in eddy CO2 flux from a Quercus ilex mediterranean forest, Global Change Biology, 10, 1460–1469, https://doi.org/10.1111/j.1365-2486.2004.00819.x, URL `https://doi.org/10.1111%2Fj.1365-2486.2004.00819.x`, publisher: Wiley-Blackwell, 2004.

Sitch, S., O'Sullivan, M., Robertson, E., Friedlingstein, P., Albergel, C., Anthoni, P., Arneth, A., Arora, V. K., Bastos, A., Bastrikov, V., Bellouin, N., Canadell, J. G., Chini, L., Ciais, P., Falk, S., Harris, I., Hurtt, G., Ito, A., Jain, A. K., Jones, M. W., Joos, F., Kato, E., Kennedy, D., Klein Goldewijk, K., Kluzek, E., Knauer, J., Lawrence, P. J., Lombardozzi, D., Melton, J. R., Nabel, J. E. M. S., Pan, N., Peylin, P., Pongratz, J., Poulter, B., Rosan, T. M., Sun, Q., Tian, H., Walker, A. P., Weber, U., Yuan, W., Yue, X., and Zaehle, S.: Trends and Drivers of Terrestrial Sources and Sinks of Carbon Dioxide: An Overview of the TRENDY Project, Global Biogeochemical Cycles, 38, e2024GB008 102, https://doi.org/10.1029/2024GB008102, URL `https://onlinelibrary.wiley.com/doi/abs/10.1029/2024GB008102`, _eprint: https://onlinelibrary.wiley.com/doi/pdf/10.1029/2024GB008102, 2024.

Van Sundert, K., Leuzinger, S., Bader, M. K., Chang, S. X., De Kauwe, M. G., Dukes, J. S., Langley, J. A., Ma, Z., Mariën, B., Reynaert, S., Ru, J., Song, J., Stocker, B., Terrer, C., Thoresen, J., Vanuytrecht, E., Wan, S., Yue, K., and

Vicca, S.: When things get MESI: The Manipulation Experiments Synthesis Initiative—A coordinated effort to synthesize terrestrial global change experiments, Global Change Biology, 29, 1922–1938, https://doi.org/10.1111/gcb.16585, URL `https://onlinelibrary.wiley.com/doi/10.1111/gcb.16585`, 2023.

Viechtbauer, W.: Conducting Meta-Analyses in R with the metafor Package, Journal of Statistical Software, 36, 1–48, https://doi.org/10.18637/jss.v036.i03, URL `https://doi.org/10.18637/jss.v036.i03`, 2010.